Chapter

Nuclear Thermal Propulsion

Mark D. DeHart, Sebastian Schunert and Vincent M. Labouré

Abstract

This chapter will cover the fundamentals of nuclear thermal propulsion systems, covering basic principles of operation and why nuclear is a superior option to chemical rockets for interplanetary travel. It will begin with a historical overview from early efforts in the early 1950s up to current interests, with respect to fuel types, core materials, and ongoing testing efforts. An overview will be provided of reactor types and design elements for reactor concepts or testing systems for nuclear thermal propulsion, followed by a discussion of nuclear thermal design concepts. A section on system design and modeling will be presented to discuss modeling and simulation of driving phenomena: neutronics, materials performance, heat transfer, and structural mechanics, solved in a tightly coupled multiphysics system. Finally, it will show the results of a coupled physics model for a conceptual design with simulation of rapid startup transients needed to maximize hydrogen efficiency.

Keywords: neutronics, high temperature, multiphysics, griffin, MOOSE, nuclear thermal propulsion, interplanetary, NASA

1. Introduction

Nuclear thermal propulsion (NTP) is a technology that uses a nuclear reactor to provide the necessary energy to power a spacecraft for extraterrestrial operations [1]. At the most basic level, nuclear thermal propulsion is simply the use of nuclear fission to heat a gas to a high exit velocity. In this sense, it is very similar to a chemical rocket, in which the exothermic reaction of hydrogen and oxygen provides the energy used to heat the reaction product—gaseous H_2O—to generate thrust. However, in an NTP engine, molecular hydrogen (H_2) is used as the propellant. The H_2 is used to remove heat from a reactor core by convection; the added energy provides a high speed exit velocity to generate thrust.

For an NTP engine using an H_2 propellant, the engine is two to three times as efficient as an H_2/O_2-fueled rocket engine. Here, efficiency is measured in terms of *specific impulse* (I_{sp}). The Isp is the amount of time (in seconds) that a rocket engine can generate thrust with a fixed Earth weight (mass $\times$ g_o) of propellant, when the weight is equal to the engine's thrust [2]. Here g_o is the gravitational constant on Earth, about 9.81 m/s^2, and relates mass to weight. For an H_2/O_2 engine, the I_{sp} is around 450 s. For nuclear thermal propulsion with H_2, the I_{sp} is approximately 900 s [3]. Hence, the United States (U.S.) National Aeronautics and Space Administration (NASA) has had a long interest in use of NTP for propulsion, with recent interest in missions to Mars between 2030 and 2050 [4], and for cislunar operations, with a plan to demonstrate an NTP system above low Earth orbit (LEO) by 2025 [5].

This chapter is organized as follows. First, background will be provided on historical NTP work and current needs for operation—specifically, the functionality of an NTP engine. Next, we will detail key components of core physics design, focusing on the nuclear subsystem of the larger plant. We will briefly discuss the balance of plant as it relates to the nuclear subsystem, then conclude with a presentation of simulation results for a conceptual nuclear thermal propulsion system.

2. Background

In this section, we will discuss the evolution of the NTP concept from its theoretical beginnings in the late 1940s to present-day needs. Much of the knowledge being applied in current NTP system design is drawn from knowledge gained through a series of experimental programs beginning in the late 1950s and running through the early 1970s. However, current interests have resulted in new materials testing based on experience gleaned from earlier work combined with modern materials performance data and testing methods. A major focus of the NASA Space Nuclear Propulsion Program is in reviving NTP fuel fabrication techniques and design knowledge [6]. Hence, an overview of the history of NTP is appropriate before moving on to current testing programs. These programs provide significant insight for current research and testing programs. But first, let us revisit the motivation for nuclear thermal propulsion over chemical engines for extraterrestrial propulsion.

2.1 Advantages of nuclear thermal propulsion for interplanetary travel

The efficiency of a rocket engine design is commonly measured in terms of specific impulse. One can think of I_{sp} as the miles per gallon or kilometers per liter for a car. The larger the I_{sp}, the more efficient the engine. Mathematically, specific impulse is defined as the total engine thrust integrated over time per unit weight of the propellant; here, weight is defined as measured on Earth (e.g., N, or, historically, lb_f) [7]). Thrust is defined as:

$$F_{\text{thrust}} = v_e \cdot \dot{m} \tag{1}$$

where:
F_{thrust} is the force (thrust) exerted by the propellant (N),
v_e is the exit velocity of the exhaust propellant (m/s) relative to the nozzle, and
$\dot{m}$, or dm/dt, is the mass flow rate of the propellant (kg/s).

The total impulse (I) of a rocket for time t is defined as the thrust integrated over the total time of operation (*burn time* in a chemical rocket, or time at power in an NTP engine):

$$I(t) = \int_0^t F_{\text{thrust}}(\tau)\,d\tau = \int_0^t v_e \cdot \dot{m}\,d\tau = m_{ex} \cdot v_e \tag{2}$$

Here, we have assumed that v_e is constant, and m_{ex} is the total mass expelled over the time of operation, $m(0) - m(t)$.

Specific impulse is defined as the total impulse divided by the weight W of the propellant on Earth, i.e.:

$$W = m_{ex} \cdot g_o \tag{3}$$

Hence,

$$I_{sp} = \frac{m_{ex} \cdot v_e}{W} = \frac{m_{ex} \cdot v_e}{m_{ex} \cdot g_o} = \frac{v_e}{g_o} \tag{4}$$

Rearranging the expressions in Eq. (1), in terms of v_e and replacing v_e in Eq. (4), we arrive at a more useful definition for I_{sp}:

$$I_{sp} = \frac{F_{thrust}}{\dot{m} \cdot g_o} \tag{5}$$

Eq. (5) shows that the I_{sp} is the ratio of thrust to the product of the mass flow rate times the constant g_o. In this form, it is clear that the I_{sp} can be interpreted as the time (in s) over which 9.81 kg (or one Newton of weight on Earth) of propellant can produce one Newton of thrust. The larger the I_{sp}, the longer the engine is able to operate with a given mass of fuel.

A pioneer in rocketry theory in the early 1890s, Konstantin Tsiolkovsky [8] derived a number of important relationships, including Eq. (6), which is used heavily in rocket design and is known as the ideal exhaust velocity equation, relating gas properties to the exit velocity of the propellant:

$$v_e^2 = \frac{\frac{2kRT_c}{M}\left(1 - \left(\frac{p_e}{p_c}\right)^{\frac{k-1}{k}}\right)}{k-1}, \tag{6}$$

where:

k is the ratio of the specific heat at constant pressure (c_p) to specific heat at constant volume (c_v) for the propellant (i.e., $k = c_p/c_v$),

R is the universal gas constant,

T_c is the reactor core exit temperature for NTP, or the combustion chamber temperature for a chemical engine,

M is the molecular weight of the propellant,

p_e is the nozzle exit pressure, and

p_c is the core exit (or combustion chamber) pressure.

R is a fundamental physical constant, k does not vary significantly between different gases (typically between 1.1 and 1.5) and T_c, p_c, and p_e depend on the engine specifications. Assuming that k, Tc, pc, and pe are known and identical between NTP and a chemical rocket, we can combine them into the constant C:

$$I_{sp} = \frac{C}{\sqrt{M}}, \tag{7}$$

For rockets that use the chemical reaction of H_2 and O_2 to produce energy and release high temperature H_2O, the atomic mass of the propellant, M, is 18 g/mole. NTP engines use high energy H_2 ($M = 2$ g/mole) that is discharged from a high temperature core. Comparing the theoretical specific impulses,

$$\frac{I_{sp}(H_2)}{I_{sp}(H_2O)} = \frac{C_{H_2O}/\sqrt{2}}{C_{H_2}/\sqrt{18}} = \sqrt{18/2} = 3. \tag{8}$$

This assumes that C_{H_2O} is equal to C_{H_2} (they are similar but not equal). Thus, based on ideal gas assumptions, H_2 could provide three times the I_{sp} of H_2O as a propellant. However, in reality, gas is not ideal and the value of C_{H_2O} is not equal to

C_{H_2}, as the value of k is not the same for the two fluids. In addition, for NTP, the most significant challenge is in obtaining a high exit temperature from the core. This requires nuclear fuel materials to be able to quickly rise to and maintain very high temperatures. Chemical engine combustion chamber temperatures are on the order of 3500 K; NTP efforts currently aim for a temperature of approximately 2700–3000 K based on material limits. Together, these facts somewhat reduce the advantage in I_{sp} from the ideal value of 3 to a ratio closer to 2. Nevertheless, with the I_{sp} for a H_2/O_2 engine is on the order of 450 s, while for NTP, it would be on the order of 900 s. Hence, there remains a clear advantage to the use of an NTP engine. Heating H_2 to significant outlet temperatures can be achieved using a nuclear reactor.

This advantage was recognized in the 1940s. An NTP-propelled spacecraft could significantly reduce the travel time to Mars as compared to conventional engines [9]. This would reduce astronaut radiation exposure, as well as the impact of the long-term microgravity environment.

Note that NTP engines are not intended for liftoff from Earth; they are not designed to provide sufficient thrust for launch. Chemical engines would be used to lift a full vessel (in parts) to low earth orbit (LEO), from where the vessel would be assembled and an NTP-propelled mission would be launched.

In the late 1960s, the well-known pioneer of modern rocketry, Wernher von Braun, then the director of the NASA Marshall Space Flight Center, advocated for a mission to Mars. Under his plan, NASA would launch a Mars mission in November 1981 (based on favorable planetary alignment), and land on the red planet by August 1982. Von Braun explained that "although the undertaking of this mission will be a great national challenge, it represents no greater challenge than the commitment made in 1961 to land a man on the moon" [10]. In the following subsection, we will briefly visit early NTP research and the Nuclear Engine for Rocket Vehicle Application (NERVA) rocket engines that von Braun had envisioned would take men to Mars.

2.2 History of nuclear thermal propulsion

The concept of nuclear thermal propulsion was first publicly published by the Applied Physics Laboratory in 1947 [11]. Development of NTP systems began at Los Alamos Scientific Laboratory (LASL) in 1955 as Project Rover, under the auspices of the Atomic Energy Commission (AEC). NASA was formed in 1958 in response to Russia's launch of Sputnik and the beginning of the space race, and took over the Rover project with continued collaboration with LASL and the AEC [12]. Rover later became a civilian project within NASA and was reorganized to perform research directed toward producing a nuclear powered upper stage for the Saturn V rocket. In 1961, the NERVA program was formed by NASA to develop a nuclear thermal rocket engine. The program designed, assembled, and tested 20 nuclear rocket engines through a number of experimental series, including the KIWI, PEWEE, PHOEBUS, TF, and NRX reactors. These ground-based test reactors used solid fuel, based on advanced graphite materials, and were thermal spectrum reactors. The NRX-XE rocket reactor performed 28 burns with more than 3.5 h of operation [6], demonstrating the ability to operate and restart with the high performance requirements needed for use in an NTP system.

A Nerva-type engine concept is depicted in **Figure 1**. The fuel is manufactured as solid hexagonal blocks, with holes drilled through for hydrogen flow to cool the core. Multiple elements are assembled to create the core, with criticality control through the use of control drums with a poison plate on one side of the cylindrical drum, much as has been used at the Advanced Test Reactor (ATR) for over 50 years [14]. Minimal excess reactivity is needed as the total core lifetime will be on the order of hours, and will only operate for times on the order of an hour or less

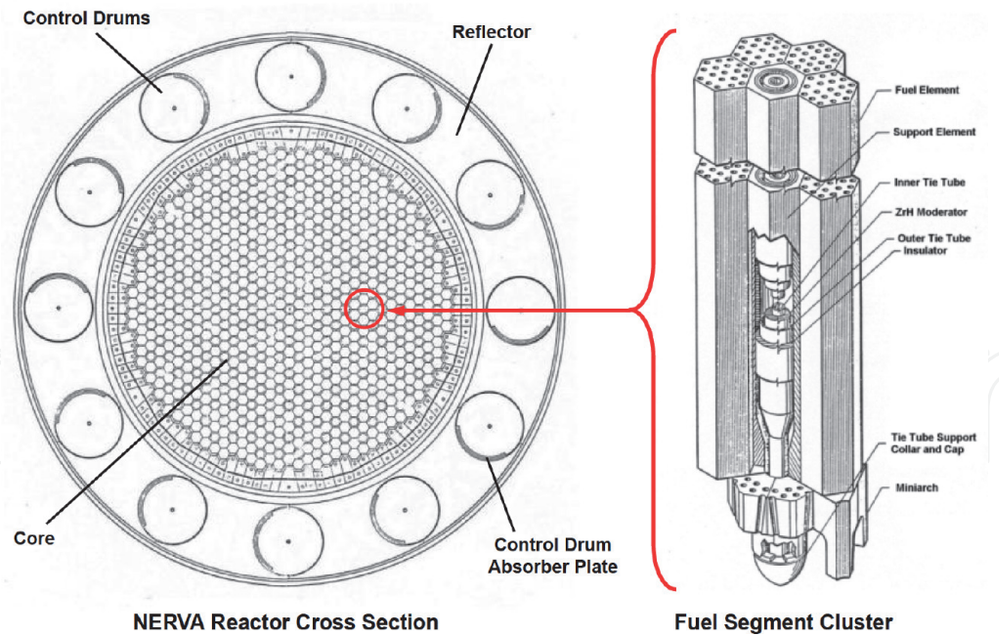

Figure 1.
Reactor core cross section for a ROVER-type NTP engine (left) and a cutaway of a fuel assembly cluster (right) [13].

resulting in minimal xenon buildup. These reactors were fueled using high-enriched uranium (HEU) in excess of 90% ^{235}U.

Both the Rover and NERVA research focused on a fuel form consisting of a graphite matrix with dispersed fuel (GMWDF). Graphite fuel compacts were used with various fuel types, including UO_2 and UC_2 fuel particles, and as (U,Zr)C[1] graphite composite. The three fuel forms used with the GMWDF compact are [15]:

- *Particles in graphite matrix:* This is the earliest compact form. It first contained UO_2 particles that were later replaced by UC_2 particles. This compact did not retain fission products and was soon abandoned.

- *Pyrolytic carbon (PyC):* PyC coated particles in a graphite matrix are the second generation of fuel used in the Rover and NERVA programs. This compact used UC_2 fuel particles and retained fission products well, but it features an inferior structural integrity as compared to the (U,Zr)C composites.

- *(U,Zr)C composite:* This is the most advanced of the GMWDF compacts with good structural integrity, closely matching thermal expansion coefficients between the composite and ZrC coating, as well as additional protection against corrosion by the carbide composite layers.

GMWDF compacts lead to a hard thermal spectrum [16–18]. Early designs exclusively used the graphite matrix as a moderator, but later designs starting with the PEWEE 1 experiment included ZrH sleeves in tie rods to increase the moderation ratio and reduce the core size [17]. The main issue with GMWDF compacts is that hot hydrogen corrodes the graphite matrix if they come into direct contact [15]. Therefore, all GMWDF compacts used coatings to protect the graphite matrix. The coatings must match the thermal expansion of the matrix closely to avoid excessive cracking. While still remaining a concern at the conclusion of project NERVA, corrosion rates were reduced by more than a factor of 10 [17]. GMWDF was used in

[1] This notation denotes a solid solution where C sits on one lattice and U and Zr share the second lattice.

the shape of fuel plates (KIWI-A) and cylindrical fuel elements in a graphite module (e.g., KIWI-A′ and KIWI A3), but most often as hexagonal fuel elements connected via tie tubes [17], as illustrated in **Figure 1**.

While not used in most early testing, CERamic-METallic (CERMET) fuels were evaluated during the NERVA program. The technology was too new and not well understood in the early 1960s, but was being investigated in parallel to the NERVA experiments. CERMET compacts consist of ceramic fuel particles embedded in a refractory metal matrix [19, 20]. The choice of matrix and fuel material influences thermal stability, thermal conductivity, structural integrity, and neutronics performance of the CERMET compact. Concurrent with the NERVA program, ANL and General Electrics (GE) developed separate CERMET NTP concepts. In a simplistic sense, CERMET fuels are particles of ceramic fuel (i.e., UO_2 or UN) encapsulated in a metal matrix, typically, but not limited to, tungsten, rhenium, or molybdenum. The research conducted by ANL and GE included the development and testing of the CERMET fuel and the design of the ANL-200, ANL-2000 [20, 21], and the GE 710 reactors [21, 23]. These CERMET programs focused entirely on HEU fuel kernels and fast reactor concepts. In contrast to GMWDF, the GE CERMET concepts did not undergo prototypical irradiation testing, nor did either concept undergo engine testing. Therefore, prior to the twenty-first century, the technology readiness of CERMET compacts trailed that of the GMWDF compacts.

The matrix material of a CERMET usually makes up about 30–60% of the compact volume [23], so its properties are both neutronically and structurally important. The ANL and GE programs focused mostly on natural tungsten as matrix material [20]. Among the available matrix materials, tungsten provides the largest fracture strength and temperature stability [6]. However, tungsten is brittle at low temperatures, causing issues with cracking. All isotopes of tungsten have strong (n, γ) resonances between 1 eV and 5 keV, thereby making tungsten neutronically challenging, except for fast reactor applications.

Fuel kernels also make up a significant fraction of the volume, so the materials properties and performance must be evaluated. Some work was performed in this area under the GE and ANL engine design programs for UO_2 and UN fuel types, as described below:

- *UO_2:* UO_2 fuel kernels were the only fuel form used in the ANL program and the primary fuel type pursued in the GE 710 project [15]. UO_2 has a uranium density of 9.7 g/cm^3. Both the ANL [20] and GE 710 programs used HEU enriched to 93%. For HEU CERMET compacts, the uranium content of the ceramic phase is not as important because enrichment can be adjusted to provide sufficient fissile material. The thermal conductivity of UO_2 is about 10 W/mK at room temperature and reduces with increasing temperature and burnup [24].

- UN: UN fuel kernels were considered as part of the GE 710 project [15]. UN has a uranium density of 10.7 g/cm^3. The thermal conductivity of UN is larger than that of UO_2 starting with a thermal conductivity of roughly 14 W/mK and increasing with temperature [25].

The GE experiments were at temperatures significantly lower than the NTP requirements, but provided much data on materials behavior and failure mechanisms [20, 26]. ANL focused on the production of CERMET fuels; different fuel fabrication procedures were employed with mixed success. Non-nuclear testing of samples was performed in flow loops of hydrogen heated to 2770°C to understand the fuel loss rates. Nuclear tests on the ANL CERMET samples were run in the Transient Reactor Test Facility (TREAT) located at Idaho National Laboratory

(INL). Eight specimen CERMET fuels, each with seven coolant holes, were tested under pulsed reactor conditions. Some fuel failure was observed in a few of the experiments [20, 26, 27].

With the success of the missions to the moon and the space race won after putting a man on the moon, the U.S. changed priorities for space exploration. Along with the cancelation of the Apollo missions, the NERVA program was terminated in 1972. Nevertheless, these programs provided a wealth of experience and knowledge; this work has been recently resurrected. Although the basics of rocket science have not changed since the 1970s, our understanding of materials performance and the development of new fabrication processes have advanced.

2.3 Current testing for NTP materials

Although historical experience in NTP design has provided a wealth of valuable data, recent advances in materials research have somewhat altered approaches to the design of NTP fuel, especially with respect to fuel material compositions, fabrication, and testing. Programs described earlier used HEU; current design concepts are based on high assay low enrichment uranium (HALEU) with a ^{235}U enrichment of less than 20% (often also referred to as simply LEU). Working with LEU greatly reduces security concerns and allows existing NASA facilities to work with fuel samples with minor modifications to address radiological concerns. HALEU would also be available at a significantly lower cost than that of HEU, and is much easier to transport. At the time of this writing, NASA is working with existing feed stock for test specimens as the U.S. cannot currently produce HALEU fuel. However, in June 2021, the U.S. Nuclear Regulatory Commission (NRC) approved a request from Centrus Energy to produce HALEU fuel at its enrichment facility in Piketon, Ohio. Centrus has already built 16 centrifuge machines for uranium enrichment, expecting to begin HALEU production by early 2022 [28]. This fuel will be used by both NASA and a number of advanced reactor prototypes under development in the U.S.

Current research and development efforts are organized within NASA's Space Technology Mission Directorate and are focused on both fabrication and performance under prototypical conditions. Although no NTP engine prototypes have been developed since the earlier work in Rover and NERVA programs, other facilities have been used for materials testing under reactor conditions. In early 2015, the first partial-length fuel elements were tested in the Nuclear Thermal Rocket Element Environmental Simulator (NTREES) located at NASA's Marshall Space Flight Center (MSFC) [29]. NTREES has been designed to provide up to 1.2 MW of heating to simulate an NTP thermal environment by capturing exposure to hydrogen heated to temperatures up to more than 3000 K. Numerous tests have been completed in NTREES; however, the facility is non-nuclear and unable to produce the intense neutron and gamma fluxes that will be present in an NTP engine. To that end, a number of tests have been completed or are planned for high-power transient tests in TREAT. In June 2019, the experiment designated as SIRIUS-CAL was the first test of an NTP-type fuel specimen. As with NTREES, a number of tests with representative fuel specimens have been completed and are ongoing.

To date, tests have been performed using CERMET fuel specimens based on fabrication experience gained in earlier ANL and GE CERMET tests, along with other facility tests. About 200 CERMET samples were tested in the various programs by thermally cycling to high temperatures in hydrogen [6], providing valuable data for performance and fabrication. CERMET fuel also allows for considerable control in fabrication due to the unique structure of the material itself.

Building on the earlier experience with natural tungsten as a matrix material, new materials have been evaluated:

- *Enriched tungsten:* Identical to standard tungsten, except that it is enriched in ^{184}W. While all isotopes of tungsten have strong (n,γ) resonances, ^{184}W has the least pronounced resonances with cross-sections smaller than 1000 barns and confined to energies between 10 and 500 eV.

- *Rhenium alloyed tungsten:* Rhenium increases the compact's ductility [15], but may reduce temperature limits [15].

- *Molybdenum:* Molybdenum compacts are more ductile than tungsten compacts, but are less heat resistant (e.g., they have a higher vapor pressure than tungsten) and prone to significant swelling induced by fission gas release [30]. Molybdenum has strong (n,γ) resonances between 10 eV and 50 keV that make it as neutronically challenging as tungsten.

- *Molybdenum-30 wt% tungsten:* Mo-30 W is of interest for moderated, LEU NTP reactors [31]. Mo-30 W is a good compromise between tungsten and molybdenum because its density is smaller, while its durability is just slightly below pure tungsten.

CERMETs can be used in LEU designs as discussed in Refs. [23, 32]. However, parasitic absorption of tungsten and ^{238}U, as well as reduction in fissile content, make it impossible to build a CERMET-based fast spectrum LEU core using natural tungsten [33]. Thus, the current focus of CERMET LEU cores is on thermal spectrum systems [23, 32]. For thermal reactors, CERMET offers the advantage of a higher fuel density as compared with composite GMWDF. However, the neutronic behavior of a CERMET compact is challenging because of parasitic absorption, the lack of moderating ability, and a short mean free path for the thermal neutrons [23]. These challenges result in difficulty adding reactivity to the core, requiring large fuel loadings and effective reflectors. They also exhibit significant self-shielding across fuel elements (with NERVA dimensions), leading to intra-element peaking and non-uniform burnup distributions after several tens of hours of operation [23].

NASA has been pursuing a parallel path in evaluation of CERMET- and CERCER (CERamic–CERamic)-based fuel forms. In 2021, NASA decided to place more emphasis on CERCER-based fuel concepts moving forward, although a number of CERMET-based fuel experiments are in the testing pipeline for the next few years. As opposed to CERMET, CERCER fuel requires approximately seven times less HALEU, has lower maximum fuel meat stresses, and is lighter [34]. CERCER fuels with coated fuel particles also offer the potential for increased margins with respect to fuel matrix melting compared to CERMET systems, but are at a lower level of technological and fabrication maturity. CERMET fabrication and testing began in the 1960s and 1970s for NTP applications, while CERCER (in NTP applications) is a relative newcomer [35]. The fabrication processes of CERCER fuels is currently based on relatively simple compression and sinter methods.

Both CERMET and CERCER fuels are being tested at both the TREAT and NTREES facilities. **Figure 2** illustrates the current plan for the experiments at TREAT with both CERCER and CERMET for the next several years. The CERMET tests have served as a technology pathfinder for CERCER fabrication and testing methods. The figure also shows the current plan for the testing program at TREAT, with experimental configurations becoming more complex, as well as plans to migrate from CERMET to CERCER fuels.

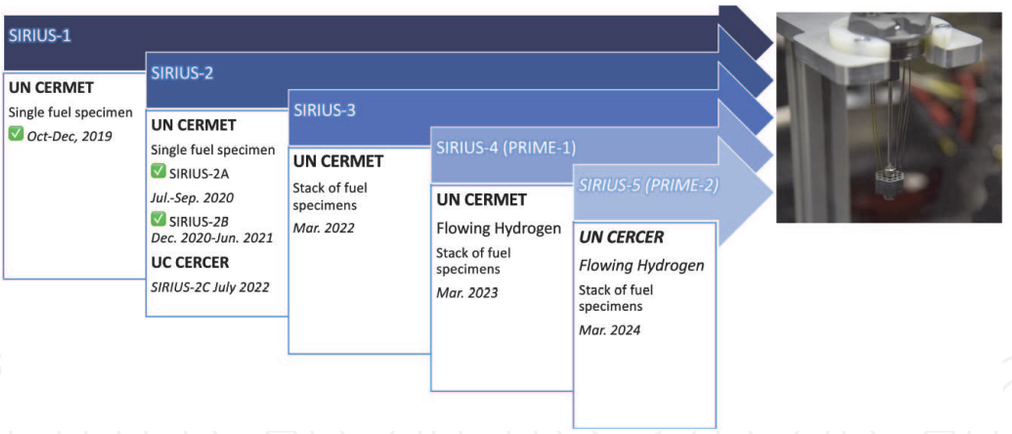

Figure 2.
Current high power neutronic testing plans; picture on the right shows the SIRIUS-1 test specimen being prepared for irradiation testing.

2.4 Needs for nuclear thermal propulsion material testing

The tests described in the previous section are being performed to collect information on the performance limits of fuel forms and cooling configurations. To meet mission requirements, it is desirable to maximize fuel temperatures, but higher temperatures introduce other issues: expansion, stresses, Doppler broadening, and chemical interactions. For the latter, early graphite fuel experiments under Rover highlighted the need to use coatings on the fuel grains. It is also known that fuel hydration from direct contact between fuel and hydrogen coolant has a deleterious effect on fuel performance [36]. Test specimens often include cladding materials on flow surfaces, which requires an additional evaluation in terms of clad/fuel interactions. Cladding is also an additional challenge in fuel fabrication. Cycling of the fuel from zero power to high power, operation at steady state for tens of minutes, and the return to zero power results in the potential buildup of temperature-driven stresses, which could ultimately lead to failure. Hence, material testing must address all of these physics, either in integral or separate effects testing. Both TREAT and NTREES provide capabilities for such tests. NTREES allows for larger specimen sizes and (until the SIRIUS-4 experiment is fabricated) is the only facility that provides for high temperature hydrogen flow. TREAT allows for direct nuclear testing with energy distributions that would be more typical of an NTP configuration. However, hydrogen flow within fuel specimens will be introduced within TREAT with the first Prototypic Reactor Irradiation for Multicomponent Examination (PRIME) experiments. PRIME-1 (also known as SIRIUS-4) will use CERMET fuel, while PRIME-2 will repeat the experiment with a CERCER fuel sample. Both are shown on the timeline in **Figure 2**. After PRIME-2, further experiments will focus on the evaluation of CERCER fuel specimens.

3. Overview of reactor types for NTP

A plethora of different NTP reactors were proposed and some of them were tested. Before considering particular examples, distinguishing features of reactor types are discussed. This allows for the development of a taxonomy of NTP reactors where one can more easily appreciate the differences in reactor physics characteristics and performance. We discuss different neutron spectra, fuel element geometry concepts, the use of low enriched and highly enriched uranium, fuel compact type, and the interplay of these factors when considering example designs.

3.1 Impact of the neutron spectrum

The advantage of thermal spectrum reactors is that criticality can be achieved with less fissile material in the core. In turn, the advantages of fast reactors are that no moderator is necessary, thereby allowing more space for fuel, and that the fuel matrix can be constructed from refractory metals without suffering from parasitic absorption at small neutron energies. Fast reactor designs are simpler and more robust because there is no need for a moderator that is either sensitive to elevated temperature, hot hydrogen, or both. In addition, the technological challenges of startup are smaller for fast reactors because of the smaller temperature defect and H_2 worth [37]. Finally, flooding with water leads to negative feedback effect in fast reactors [22].

Fast spectrum NTPs during the ANL-200/2000 and GE-710 projects were designed using HEU CERMET in hexagonal assemblies. It is impossible to achieve criticality in a fast reactor with LEU CERMETs [33]. However, it is possible to design a core with sufficient excess reactivity using UN fuel plates with refractory metal cladding [33]. This is enabled by the much smaller ratio of refractory metal to fuel volume than in the LEU CERMETs.

3.2 Neutronics parameters of interest

The moderator-to-fuel density ratio (MTFR) [38] is an important characteristic for the reactivity of a reactor. There exists an MTFR at which the core multiplication factor assumes a maximum and the core is optimally moderated, while for smaller or larger MTFRs, the core is undermoderated or overmoderated, respectively. From a control perspective, it would be desirable to have an undermoderated core to avoid positive feedback from increasing power. For overmoderated reactors, reduction in hydrogen density caused by an increase in power can lead to a positive reactivity feedback loop. NERVA and derived designs are all undermoderated, as the addition of hydrogen leads to an increase in core reactivity [39]. For LEU reactors, multiplication factor, size, weight, and thermodynamic performance depend heavily on the moderator-to-fuel ratio [40].

Power peaking measures how uniformly the power is produced in the core, and can be computed by taking the maximum power density observed in the reactor and dividing it by the average power density [41]. In practice, it is more common to consider fuel element or fuel assembly peaking, and considering both axial and radial components. These are computed by taking the maximum fuel element power and dividing it by the average fuel element power. The importance of the power peaking is that limiting core conditions, such as peak temperatures, are usually experienced in peak fuel elements.

The temperature peaking factor is related to the power peaking factor, but is influenced by both the power peaking and thermal-fluid conditions in the core. It is defined as the peak fuel element temperature divided by the average temperature of the fuel compacts. Larger power peaking factors can be addressed by directing more flow to the high-power regions, which leads to reduced temperature peaking factors.

Reactivity feedback is the effect that non-neutronic parameters have on the reactivity of the core. When reactivity is positive, reactor power increases, while the opposite is true for negative reactivity. The most important feedback mechanism and the parameters to which they are sensitive are:

- *Doppler Broadening:* Doppler broadening increases the absorption by increasing resonance width with increasing material temperature [38]. While any

material with absorption resonances exhibits Doppler broadening, the most prominent effect is usually stemming from ^{238}U. Due to the much larger amount of ^{238}U relative to HEU, Doppler broadening is much more important in LEU reactor concepts. Doppler broadening is always a negative feedback effect with increasing temperature and is effectively an immediate effect with respect to the temperature of the fuel.

- *Spectral Shift:* Spectral shift refers to the hardening of the spectrum when the moderator temperature is increased. Spectral shift has a negative feedback effect in graphite moderated HEU compacts [42]. However, spectral shift in reflectors can improve reflector efficiency and increase reactivity.

- *Thermal Expansion:* Thermal expansion of the core occurs due to an increase in the core temperature. Thermal expansion leads to an increase in surface area for the fuel in the core, increasing leakage at the expense of fission. Thermal expansion is sensitive to material temperatures in the core, the mechanical design of the core and the expansion coefficients of the materials. Thermal expansion is always a negative feedback effect.

- *Hydrogen Moderation:* Hydrogen in the core moderates neutrons and leads to a softer spectrum; hence, the probability of fission ^{235}U increases, while the likelihood of resonance absorption and leakage decreases. Therefore, increased hydrogen flow is usually a positive feedback effect. However, if the core is already past its optimal moderator-to-fuel ratio, the addition of more hydrogen leads to an increase in parasitic absorption in the moderator, and consequently, a reduction in reactivity.

- *Fuel Burnup:* Fuel burnup is the consumption of nuclear fuel and the production of direct and indirect fission products. It influences the reactivity by removing fissionable material and adding potential absorbers. The effect of burnup is very slow, on the order of the lifetime of the NTP system.

Fast reactors have the smallest feedback coefficients. Burnup and hydrogen content do not have an appreciable effect, while temperature via expansion and Doppler and spectral shift have a comparatively small and equal effect. HALEU-fueled reactors react predominantly to temperature via the Doppler/spectral shift. Burnup affects reactors with smaller loading of fissile isotopes more than reactors with higher fissile loading (e.g., GWDF typically has a smaller fuel loading than CERMET). The largest feedback effect for HEU GWDF is the hydrogen content of the core because Doppler broadening effects are small and the spectral shift is not as strong a feedback mechanism as that of hydrogen. Note that the sensitivity of the reactor to hydrogen content is used to introduce positive reactivity into the core by increasing the flow. The large positive reactivity coefficient does not make the HEU GWDF core dynamically unstable because an increase in reactor power leads to a reduction in hydrogen density, and thus, a negative feedback effect. Note that many observations here are based on feedback effects tabulated in Ref. [37].

Feedback is important for the controllability of the core. Large negative feedback coefficients as present in LEU cores with respect to fuel temperature require the control mechanism to have sufficient excess reactivity in reserve; therefore, thermal NTP reactors, especially if LEU fueled, must have control mechanisms with a much larger magnitude of reactivity relative to fast systems.

3.3 Geometrical arrangements

This section introduces different criteria to distinguish and classify geometries in NTP reactors. The criteria we use to distinguish these reactors are the fuel element geometry (e.g., hexagonal, annular, plates), the structural concept (tie tube or monolith), and if the moderator is heterogeneous or homogeneous. Here we compare U.S. NTP designs to concepts evaluated in the Soviet Union and the Republic of Korea. The Soviet Union began at about the same time as the Rover program, but ended in 1989 with the collapse of the Union of Soviet Socialist Republics (USSR). The Korean concept is still under active development, beginning in 2013.

NTP reactors are distinguished by their fuel element layout. The original NERVA design used hexagonal fuel elements arranged in a hexagonal lattice, as shown in **Figure 3(a)** and **(b)**. A group of six fuel elements is connected to a tie tube. The tie tube is relevant both for moderation and structural integrity as discussed below. The ratio of the number of fuel elements and tie tubes in the lattice is an important parameter for NERVA-type designs.

Fast reactor concepts originating from the ANL and GE projects also use hexagonal fuel elements, as observed in **Figure 3(c)**, arranged in a hexagonal lattice, as seen in **Figure 3(d)**, but the fuel elements tend to be larger than their NERVA counterparts and contain more coolant channels. The hexagonal fast concepts do not require tie tubes.

The Russian NTP program considered a variety of fuel element shapes (see Ref. [15]) among which the twisted ribbon design depicted in **Figure 3(e)** was selected as the most promising option. Usually, each twisted ribbon is referred to as a fuel element; it should be noted that each twisted ribbon is significantly smaller than a NERVA fuel assembly. Twisted ribbons are inserted into a fuel bundle that is wrapped by insulating material. The fuel bundle is in turn inserted into a fuel assembly that is then placed into the core.

The Korea Advanced NUclear Thermal Engine Rocket (KANUTER) fuel assembly design is depicted in **Figure 3(f)**. The fuel shown in red in the figure consists of wavers forming square flow channels; interlocking of the fuel wavers forms a square lattice [45]. The fuel is surrounded by insulating carbon wrappers and a metal hydride moderator. The fuel assemblies in the KANUTER core are arranged in a hexagonal pattern.

The recent NASA/BWXT design is depicted in **Figure 3(g)** with the progression from the smallest to largest part from left to right in the figure. Each fuel element is cylindrical with round flow channels and is surrounded by an insulator. The flow channels in each element are arranged in cylindrical clusters in CANDU reactors (i.e., one central hole and six flow channels placed on a circle around the center with 12 flow channels placed on a larger circle surrounding those, etc.). The fuel elements are wrapped with structural support and then placed in holes bored through the monolithic core structure, as observed in the second picture from the right in **Figure 3(g)**. The monolithic core structure is made up of a metal hydride moderator. The fuel elements in the monolith are arranged in a cylindrical cluster, just as the coolant channels are arranged in the fuel element.

The core geometry can be distinguished by the structural support concept for the fuel elements. In the NERVA designs, a tie tube is connected to the six fuel assemblies around it, and a spring keeps the fuel elements in tension to avoid damage to the core structure by flow-induced vibrations and support the core against the axial pressure drop [47]. The tie tubes are connected to a support plate located at the cold end of the core. Additional axial support is provided by pedestals in some reactors (e.g., PEWEE) [17].

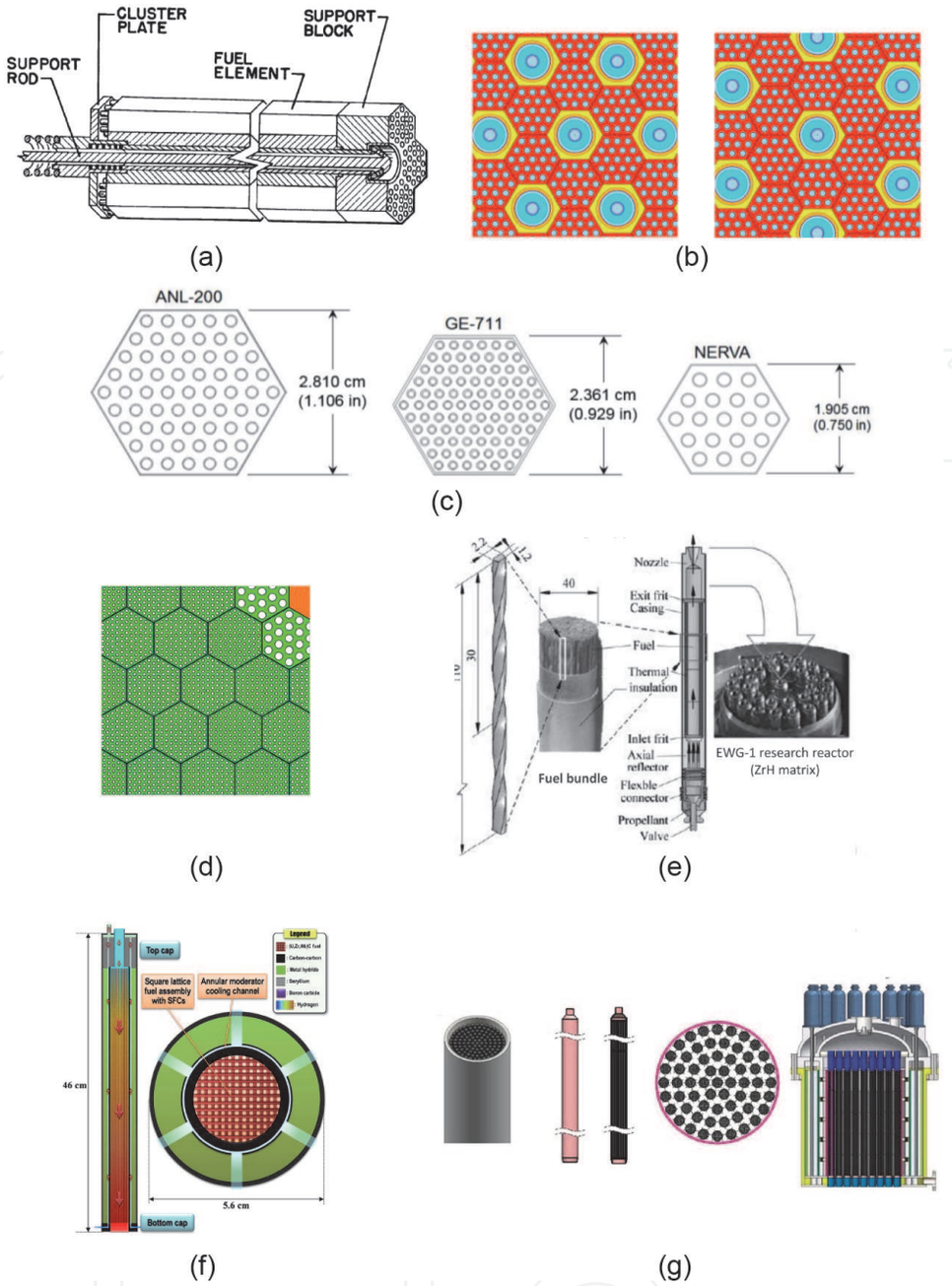

Figure 3.
An overview of the geometric arrangement of different NTP concepts. (a) Typical later NERVA fuel element layout. Six fuel elements are connected to a tie-tube [16]. (b) NERVA hexagonal fuel element layout with a different ratio of tie-tube and fuel elements [43]. (c) ANL-200, GE-711, and NERVA fuel assembly geometries [44]. (d) Hexagonal lattice of fuel elements typical for fast reactor designs like ANL-200 and GE-710 [32]. (e) Russian NTP concepts using a twisted ribbon fuel element in an encased assembly that is inserted into the reactor (picture (e) from left to right) [39] (length units are mm). (f) Korean integrated fuel assembly design with square flow channels [45]. (g) Recent "fuel assemblies under consideration for NASA's nuclear thermal propulsion reactor designs" by BWXT advanced technologies, LLC [46].

In contrast to the tie tube design, the more recent NASA/BWXT design uses a monolith concept, as described in Ref. [46] and shown in **Figure 3(d)**. The monolithic core structure is made up of the metal hydride moderator and has borings that contain the fuel assemblies. The fuel elements are wrapped with insulator and structural support. The structural support is fastened to a support plate at the cold end of the core. Additional axial support at the cold end may be included in the design as well.

Finally, the KANUTER design, as shown in **Figure 3(f)**, arranges beryllium spacers between the integrated fuel assemblies. In contrast to the NASA/BWXT

design, the integrated fuel assemblies contain a moderator where the core support structure is strongly moderating.

Reactors can also be classified by how the moderator and fuel are arranged. If the fuel and moderator are spatially separated, the reactor is *heterogeneous*; if the fuel and moderator are mixed, then the reactor is *homogeneous*. For this distinction, spatially separated means that there is sufficient distance on the order of a mean free path between the fuel and the moderator. Heterogeneous cores offer an advantage in reactivity over spatially homogeneous cores; the effect is sometimes referred to as fuel lumping. If the moderator is spatially separated from the fuel, then moderation happens away from the fuel, reducing the likelihood of resonance absorption during the slowing down process [48].

To the knowledge of the authors, the only truly *homogeneous* cores were early NERVA designs before PEWEE 1. In these designs, the moderator was the graphite matrix containing the fuel particles. Starting from PEWEE 1, the tie tubes were equipped with ZrH sleeves adding additional moderation to the system and making these designs essentially *mixed* moderation cores [17]. The Russian cores and KANUTER are *mixed* moderation cores due to the presence of graphite in the fuel compact (i.e., the homogeneous portion) and an additional moderator either in the fuel assembly or the structural components surrounding them. The recent NASA/BWXT design is a *heterogeneous* core because the only significant amount of moderator is in the monolith outside of the fuel assemblies. Fast reactors do not fall into this classification because they do not contain a moderator.

The following section discusses a small selection of representative NTP reactor concepts and provides more detail on each design.

3.4 Reactor concepts

PEWEE-1 is a demonstration reactor tested in the NERVA program in 1968 toward the end of the program. It is a small reactor when compared with the preceding Phoebus tests with power reduced from 4000 MW in the Phoebus-A design to about 500 MW [17]. To offset the increased leakage from the smaller core size, ZrH sleeves were inserted into the standard tie-tube concept of the NERVA program; the tie-tube ratio (TTR)[2] was increased and the reflector thickness was increased. The main objective of PEWEE-1 was to serve as a test bed for fuel elements and no attempt was made to maximize the outlet temperature [17]. Despite these differences to other tests within the NERVA project, PEWEE-1 is a good example of the technology used and resulting observed performance during NERVA.

In two different works [49, 50], Kotlyar focuses on studying the design space of thermal LEU-CERMET NTP concepts. These designs use the NERVA structural concept of fuel elements and tie tube/moderating elements without changing their size and shape (i.e., a hexagonal lattice with 1.905 cm flat-to-flat distance). However, the matrix is changed to LEU UO_2 particles in W-CERMET [49] and LEU UN particles in Mo or MoW-CERMET [50]. In order to overcome the reactivity penalty of refractory metals, lower uranium enrichment, and the lack of moderation in the fuel compact, Kotlyar's core concepts include significantly more moderating elements (>50% depending on core size) than PEWEE-1 with more ZrH moderator and additional carbon per moderating element. The spectrum is more thermal than in the NERVA engines, but is significantly undermoderated for the optimal small, medium, and large NTP designs [49].

[2] The ratio of tie-tube elements to total number of elements.

KANUTER [45] is unique among modern NTP designs because it uses HEU with an enrichment of 93%. The goals of the design are to maximize I_{sp}, thrust-to-weight ratio, and allow for bimodal operation (e.g., thrust and electricity generation). The NTP design uses a tricarbide (U,Zr,Nb)C fuel matrix that was tested during the Russian NTP program. KANUTER uses an integrated fuel assembly concept; the fuel assembly depicted in **Figure 3(f)** contains both fuel and a ZrH moderator that are separated by carbon–carbon insulation. The fuel matrix is arranged in wafers and the coolant channels are square. In the core, the 37 fuel elements are arranged in a hexagonal lattice and held in place by cooled beryllium spaces.

Poston [32] investigated how the performance characteristics of NTP systems change when the fuel matrix is changed from GWDF to CERMET and the enrichment is changed from LEU (19%) to HEU (93%). The four variants discussed in Ref. [32] are thus HEU-composite (e.g., NERVA carbide composite fuel), LEU-composite, LEU-CERMET, and HEU-CERMET. All concepts use hexagonal assemblies, but the assembly sizes differ: the HEU-composite uses the standard NERVA 19-hole element with a 1.91 cm flat-to-flat, the LEU-composite uses a 37-hole fuel element with a 2.77 cm flat-to-flat, the HEU-CERMET uses an element similar to the GE-710 designs with 91 holes and a 2.57 cm flat-to-flat, and the LEU-CERMET uses a 61 hole assembly with a 2.52 cm flat-to-flat. With the exception of the HEU-CERMET, all designs use the traditional fuel element/tie-tube concept of NASA albeit at different TTR (33% for HEU and LEU composite and 50% for LEU-CERMET). All concepts have an epithermal spectrum except for the HEU-CERMET. Moderation in the epithermal concepts is provided by the composite and by ZrH in the tie tubes; the LEU-CERMET requires more tie-tubes to increase the amount of moderator in the core. The CERMET in Poston's study is enriched to remove the highest absorbing isotopes from tungsten, molybdenum, rhenium, and zirconium; tungsten is used as a matrix material in the study. All designs use a Be radial reflector and the CERMET designs use a BeO top (cold-end) reflector. The performance difference and differences in the design parameters depend most heavily on ^{235}U densities. The neutronics design ensures a 1% beginning of life reactivity margin and a shutdown margin of 5%; however, LEU-CERMET barely achieves the beginning of life margin.

In Ref. [33], Youinou evaluates alternative designs to the monolithic ZrH moderated, CERMET, or CERCER concepts of the early 2020s by NASA. While several different concepts of this report deserve attention, the most important design is an LEU, plate-fueled, fast design. This concept uses UN fuel plates of thicknesses 0.5–10 mm, MoW or W clad of thickness 0.25–0.5 mm, square assemblies of size $8 \times 8 \times 80$ cm, and 7–49 fuel plates per assembly. There are 37 fuel elements in the core. The core has a power of 250 MW generating a thrust of 12,500 lbs. Youinou found that the smaller fraction of refractory metals in the plate design allow for fast LEU NTPs fueled with UN and clad with refractory metals.

The GE-710 NTP system is an example of an HEU, fast, CERMET-based concept that was developed concurrently with the graphite-based NERVA concepts [22]. The GE-710 program tested various CERMET matrix materials, including tungsten, tungsten-rhenium, tungsten-rhenium-molybdenum, and molybdenum-rhenium, among others [22]. All fuel elements investigated during the GE-710 are hexagonal and slightly larger than the NERVA fuel elements (e.g., 2.36 cm versus 1.91 cm flat-to-flat). GE-710 elements contain significantly more coolant channels than the NERVA elements, which increases the pressure drop through the core, but decreases the difference between the coolant and the maximum fuel temperature. Overall, the GE-710 project demonstrated excellent thermal and mechanical stability during thousands of hours of testing [51].

4. Modeling and simulation of NTPs

In this section, we focus on the modeling and simulation (M&S) needs for NTP systems from a nuclear reactor perspective, with a particular emphasis on transient modeling. INL leads the development of the multiphysics object oriented simulation environment (MOOSE) [52] that provides a cohesive framework for multiphysics analysis; MOOSE is introduced first. The needs of a transient reactor-centric M&S are introduced next, and then MOOSE applications performing transient simulations are introduced. Finally, we present the capabilities of MOOSE for a PID controlled startup transient.

4.1 Multiphysics object oriented simulation environment

MOOSE is a C++ based framework for a finite element and finite volume-based solution of partial differential equations. Its goal is to provide high-level access to the powerful finite element capabilities implemented in the libMesh library [53] and the linear and nonlinear solver technologies in PETSc [54] without having to understand multiple interfaces, manage parallel execution, or handle input/output. MOOSE is structured such that code can be reused among different research groups, facilitating the development of a multiphysics ecosystem referred to as the MOOSE herd.

The MOOSE framework provides: (1) extensible systems that perform tasks in a partial differential equation (PDE) solver and can be inherited from and used by physics applications; (2) an input/output handling system; and (3) specific internal data structures like the finite element mesh and finite element variables. Physics applications are developed on top of the framework. To date, the MOOSE repository comes with 21 modules (i.e., open-source physics implementations that are general enough to be packaged with MOOSE) including heat conduction, Navier–Stokes, and phase field. Many physics applications have been created based on MOOSE that contain either export-controlled, proprietary, or very specialized physics and require user approval and licensing.

The difference between MOOSE and traditional multiphysics nuclear engineering applications is that MOOSE is not a collection of single-physics codes connected with *glue code* [55]. MOOSE-based software applications are built using interfaces provided by the framework that are extended and specialized using inheritance. This paradigm shift away from using glue code provides many advantages, including reduction in data storage duplication, increased robustness against future compatibility issues, shared representation of geometry precludes developing a significant number of translation routines [56].

4.2 Relevant physics and simulation capability within MOOSE

4.2.1 Neutronics

Neutronics is at the heart of a reactor-centric viewpoint of NTP M&S. The neutron distribution drives the power distribution, which in turn drives temperatures and stresses in the core. In addition, the dynamic behavior of NTPs is to a significant degree driven by the neutronics feedback behavior. In contrast to most terrestrial reactors, NTPs spend a large fraction of their operating life in transient operation. Therefore, neutronics M&S for NTPs should provide a strong transient simulation capability. Traditionally, many neutronics tools are developed for steady-state (i.e., k-eigenmode calculations) or very slow transients (i.e., depletion

calculations). During a transient, temperature and thermal-fluids conditions can vary rapidly, making a tight coupling of neutronics and heat conduction mandatory. Finally, one of the control mechanisms for the ramp up to power is the rotation of the control drums. During a startup transient, the neutronics code must be able to accurately model the behavior of the control drums rotated to an arbitrary angle.

Griffin is the MOOSE-based reactor multiphysics application [57]. It is a superset of the capabilities previously implemented in Rattlesnake [56] and Proteus [58]. In the near-term, it will also provide an interface to the MC2–3 cross-section preparation capability [59]. The main distinction between Griffin and traditional radiation transport solvers is that it is designed for transient multiphysics simulations, making it an ideal candidate for NTP simulation. Griffin is a deterministic radiation transport application that provides the user with a variety of solvers for the linear Boltzmann transport equation. These solvers provide a variety of different fidelity levels ranging from zero-dimensional point-kinetics models over neutron diffusion with equivalence correction to high-fidelity S_N models [56, 57] with spatial kinetics.

Griffin is an ideal candidate for transient analysis of NTPs. It naturally couples to MOOSE's heat conduction capability, described later in Section 4.2.2, and can be either connected via a Newton scheme (full coupling) or a Picard iterative scheme (tight coupling). It provides several radiation transport methods that can be used in steady-state and transient analysis with general cross-section and geometric feedback. For transient simulations, cross sections are usually pre-tabulated and then interpolated during the transient. Griffin provides a control-drum decusping method that allows an accurate modeling of control drum motion during a transient simulation [60].

4.2.2 Heat conduction and conjugate heat transfer

The temperature distribution in NTPs is of great importance. First, it is the most important driver for neutronics feedback in thermal LEU-fueled reactors, and second, temperature values and differences (cold to hot) are large and margins to failure are typically small. During normal operation, most heat is transferred to the hydrogen via conjugate heat transfer. However, some of the heat is transferred from the fuel through the insulator and multiple gas gaps to the moderator and even to the reflector. Heat transfer through the gas is mostly facilitated by radiation. In addition to heat transfer from the fuel, some of the fission heat is deposited non-locally in the moderator and reflector; it is therefore required to model a significant portion of the core to obtain an accurate understanding of the temperature distribution in the moderator and reflector.

Heat conduction in an NTP needs to consider the change in thermal properties with temperatures. The temperatures over the time of a startup transient and at different locations within the reactor vary significantly. The material properties relevant for thermal analysis of the problem (e.g., thermal conductivity, specific heat, density) vary as a function of the temperature, thereby requiring an accurate model that can account for the temperature dependence of these properties. NTPs use a significant number of special purpose materials (e.g., porous ZrC insulator, refractory metal matrix with uranium inclusions) and the thermal properties of these materials need to be available.

Heat transfer in open spaces of the reactor (e.g., plena and exhaust nozzle) must also model thermal radiation in complex geometries. MOOSE provides heat conduction, gap heat transfer, and net radiation transfer capabilities within its heat conduction module. The material system in MOOSE has the ability to use general temperature-dependent material properties supplied as polynomial fits, lookup

tables, or customized material implemented in MOOSE source code. The BISON fuel performance code provides a variety of material models for nuclear materials [61]. BISON offers material properties for W and Mo-30W CERMETs [62].

The heat conduction module provides different interfaces for representing conjugate heat transfer. It can be applied as a boundary condition on channel boundaries or it can be lumped into a volumetric term. The coupling with the thermal-fluids code RELAP-7 [63] can be performed using a Robin-Neumann boundary or a Robin-Robin boundary strategy.

4.2.3 Thermal mechanics

Stresses in NTP systems arise from large temperature gradients, mechanical contact during transient and steady-state operation, and pressure differential over the core. The mechanical problem is a coupled problem between heat conduction, mechanics, contact, and potentially thermal-fluids. Vibrations can manifest in the solid structures that interact with fluid pressure oscillations caused by turbomachinery, flow separation, or other fluid-mechanical effects. The material properties relevant in mechanical problems include Young's modulus, Poisson's ratio, the linear expansion coefficient, and parameters describing plastic deformation, such as the yield stress and hardening law; these material properties generally depend on temperature.

MOOSE provides the capability to conduct mechanics simulations in the *tensor mechanics* module [64]. The tensor mechanics module is seamlessly able to couple with the heat conduction module, facilitating thermal-mechanics simulations. MOOSE also implements a variety of mechanical contact algorithms in its *contact* module. Finally, MOOSE allows pluggable multiphysics capabilities coupling neutronics, heat conduction, and time-dependent mechanics [65].

4.2.4 Thermal fluids and balance of plant

Nuclear thermal propulsion in its current form in the U.S. uses a HALEU-based reactor core to generate several hundred megajoules of thermal energy to heat hydrogen propellant to high exhaust temperatures for engine thrust. NERVA designs up to current engine concepts are of an *expander cycle* design; **Figure 4** shows a simplified representation of an NTP expander cycle engine.

In this design, high pressure liquid hydrogen (H_2) is pumped from storage tanks and is preheated while used to cool the nozzle, reactor pressure vessel, reflector and control drums and control drums (converting it to gaseous H_2), using the energy added to the gas to drive turbines. The exhaust from the turbine is directed to core support and shielding structures (not shown in **Figure 4**). Next, the gas passes through the coolant channels in the individual coolant block comprising the reactor core, where it is superheated to the necessary high exhaust temperatures. Finally, the gas is expanded through a nozzle with a high nozzle area ratio to generate thrust. Thrust is maximized by maximizing the gas temperature exiting the core, but current reactor material performance limits will restrict the peak temperature to something less than about 3000 K [44].

Unlike power reactors, NTP engines are expected to operate continuously for less than an hour at a time with weeks to months between burns [66]. Each operational period will consist of three phases: startup to full power, full thrust operation, and shutdown (with decay heat removal). Flow rates are matched to the reactor power according to the demands of each period. During startup, hydrogen economy requires as rapid an ascent to full power as possible through appropriate control drum rotation, and H_2 flow is used to both cool the reactor, as well as protect other

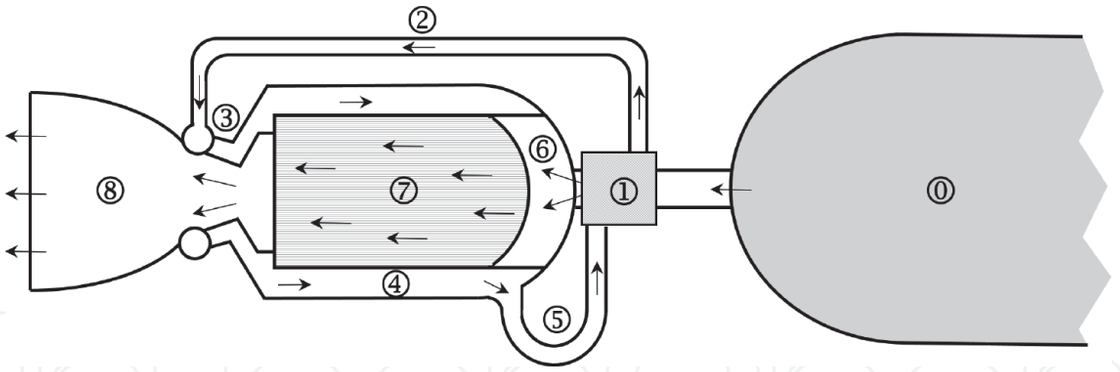

Figure 4.
Representation of NTP engine system with (0) liquid hydrogen storage tank, (1) pre-heated-hydrogen-driven turbopump, (3) nozzle cooling, (4) pressure vessel/reflector/control drum cooling, (5) gaseous hydrogen feed to turbopump, (6) gas plenum above core, (7) reactor core and hydrogen cooling, and (8) exhaust nozzle.

engine components. During the full thrust period, the core and balance of plant are near steady-state conditions. At shutdown, the reactor will be returned to a sub-critical state, but hydrogen flow will be needed for decay heat removal.

The M&S capabilities required for the thermal-fluids and balance of plant are: ability to exchange heat with solid conduction (i.e., conjugate heat transfer), modeling hydrogen in a temperature range from 40 to >3000 (or greater than 3000) K, ability to model compressible flow, availability or extendability to include heat transfer and pressure drop correlations suitable for NTPs, ability to model the relevant components in the NTP system (e.g., turbo pump and turbine on common shaft, valves, etc.), and a flexible control system that allows for the simulation of complex controllers.

RELAP-7 can solve single-phase (e.g., 3-equation model) and two-phase (e.g., 7-equation model) system analysis problems using a discontinuous Galerkin HLLC (Harten, Lax, and Van Leer Contact) discretization [67]. RELAP-7 provides models for a variety of components, including pipes, pumps, valves, and turbines; in addition, it supports both full (i.e., single nonlinear problem) and tight (i.e., Picard type) coupling with MOOSE heat conduction solvers via conjugate heat transfer. RELAP-7 provides *para-hydrogen* fluid properties across the required range, and provides a flexible and extendable control system that can be used to simulate the control system for an NTP model.

4.3 Case study of a reactor startup simulation with MOOSE

In this section, Griffin, RELAP-7, and MOOSE modules are coupled and used for a simulated startup of a LEU, CERMET-based core similar to the one depicted in **Figure 5**, but with an operating power of 250 MW and an approximate thrust of 55,600 N (12,500 lbf). The core consists of 61 LEU fuel assemblies arranged in five circular rings within a zirconium hydride (ZrH) monolithic moderator block. The startup simulation includes a PID-controlled rotation of the drums to match a predetermined reactivity setpoint curve, neutronics modeled with diffusion and Super-Homogenization (SPH) [68], heat conduction, and thermal-fluids.

From a neutronics standpoint, the probabilities of neutron interaction represented by cross-sections are affected by several temperature-driven feedback mechanisms. For the reactor shown in **Figure 5**, the primary feedback comes from the increase in ^{238}U capture reactions as the fuel heats up (Doppler feedback) while other important feedback mechanisms are spectral shift and hydrogen content in the core. From a modeling perspective, spectral shift and changes in moderator content are more difficult, because their effect is global. The value of the

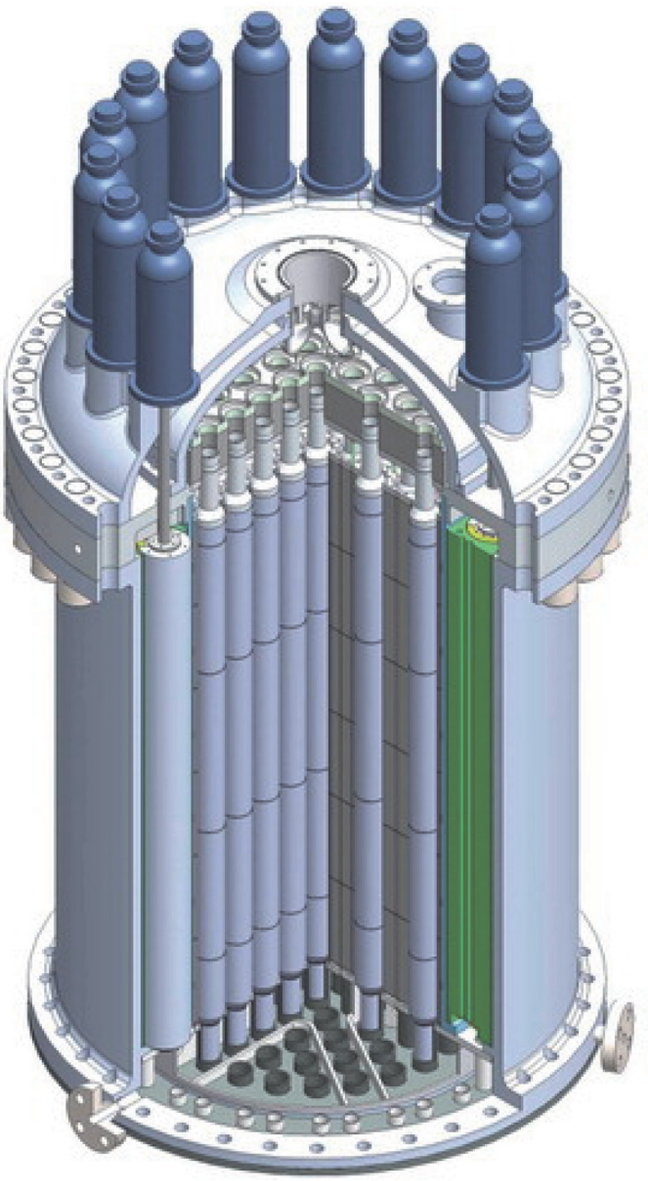

Figure 5.
Concept of BWXT NTP reactor design (picture courtesy [34]).

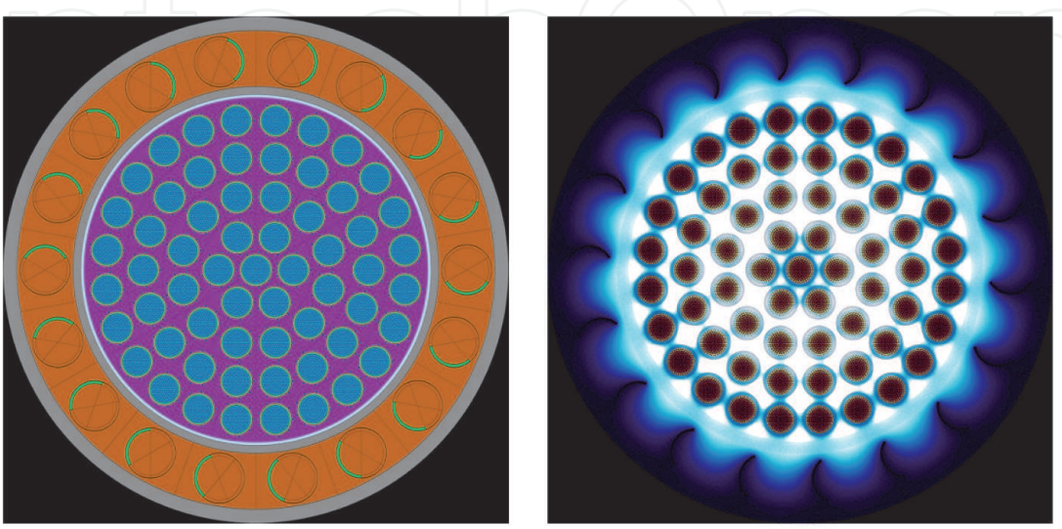

Figure 6.
Full-core serpent model. (a) Geometry; (b) fission rate and thermal flux.

temperature or hydrogen density at one point affects the neutron spectrum, and thus, the effective cross sections at another point. The distance over which non-local effects materialize depend on how far a neutron can travel without being absorbed or escape the reactor. For this kind of reactor, this travel distance, or mean free path, can be quite large (on the order of 1–100 cm, depending on the neutron energy) and complicates the cross-section evaluation significantly, especially as the tremendous axial thermal gradient gives perceptibly different neutron spectra in different parts of the core. Therefore, the analyst may opt to tabulate cross sections not only for different temperatures and hydrogen, but also for different shapes of the temperatures and hydrogen densities. For this example, cross sections are pre-tabulated for different values of the important feedback variables (e.g., fuel, moderator and reflector temperatures, control drum angle). The Serpent Monte Carlo code is used for tabulating the cross-sections for this work [69] Plots from the Serpent model are shown in **Figure 6**.

The accuracy of the solution and execution time of the model are balanced by representing the neutron distribution by the neutron diffusion equation, discretizing it on a coarse mesh, and using the full-core SPH in Griffin. SPH can be seen as a physics-based reduced order modeling approach. This enables the use of a coarse numerical mesh, as shown in **Figure 7**, while preserving the key quantities of interest needed for the multiphysics coupling, such as reactivity and power density distribution.

The moderator monolith is not expected to see a large temperature increase compared with the fuel because each of the fuel assembly is surrounded by a layer of insulator. For preliminary calculations, it is thus acceptable to assume that fuel assemblies exchange little heat with one another. Due to various symmetries, the conductive and radiative heat transfer over each ring of fuel assemblies is therefore simulated by a single 30° slice, shown in **Figure 8** and extruded over the entire height of the active core. In this figure, the orange, red, green and blue regions correspond to the fuel, insulator (ZrC), shell (SiC), and moderator (ZrH), respectively. The fuel region is penetrated by 127 cooling channels. The moderator is also cooled by flow channels to remove most of the heat that radiatively crosses the three gaps between the fuel and the moderator. The thermal-fluids is modeled by two representative cooling channels per fuel assembly ring to simulate the convective heat removal in the fuel and in the moderator.

The integration of the various sub-modules into a multiphysics model is summarized in **Figure 9**. The neutronics model provides the power density into each of the 30° slice thermal models (e.g., one per ring). These provide the wall temperature to their respective cooling channels, which in turn provide the fluid temperature and heat transfer coefficient needed to evaluate the amount of heat removed by the coolant. Once the thermal field in each of the representative fuel assemblies is obtained, the fuel and moderator temperatures are passed back to the neutronics model to update the cross sections accordingly.

To perform a reactor start-up, the control drums need to be rotated to add sufficient reactivity to not only increase the reactor power, but also compensate for the negative feedback ensuing from the heat-up of the fuel. Attempting to select the rotation of the drums *a priori* to obtain a desired power evolution would likely require significant trial and error iterations, especially considering the nonlinear behavior of the reactivity feedback coefficients and fuel heat capacity as a function of temperature. Rather, efficient control of the drums can be achieved through automated means—for instance relying on a widely-used Proportional-Integral-Derivative (PID) controller, as illustrated in **Figure 10**. Given a desired power set-point, it can be converted into a reactivity signal ($\tilde{\rho}$ in **Figure 10**), which is then compared to the *measured* reactivity from the model. This measurement

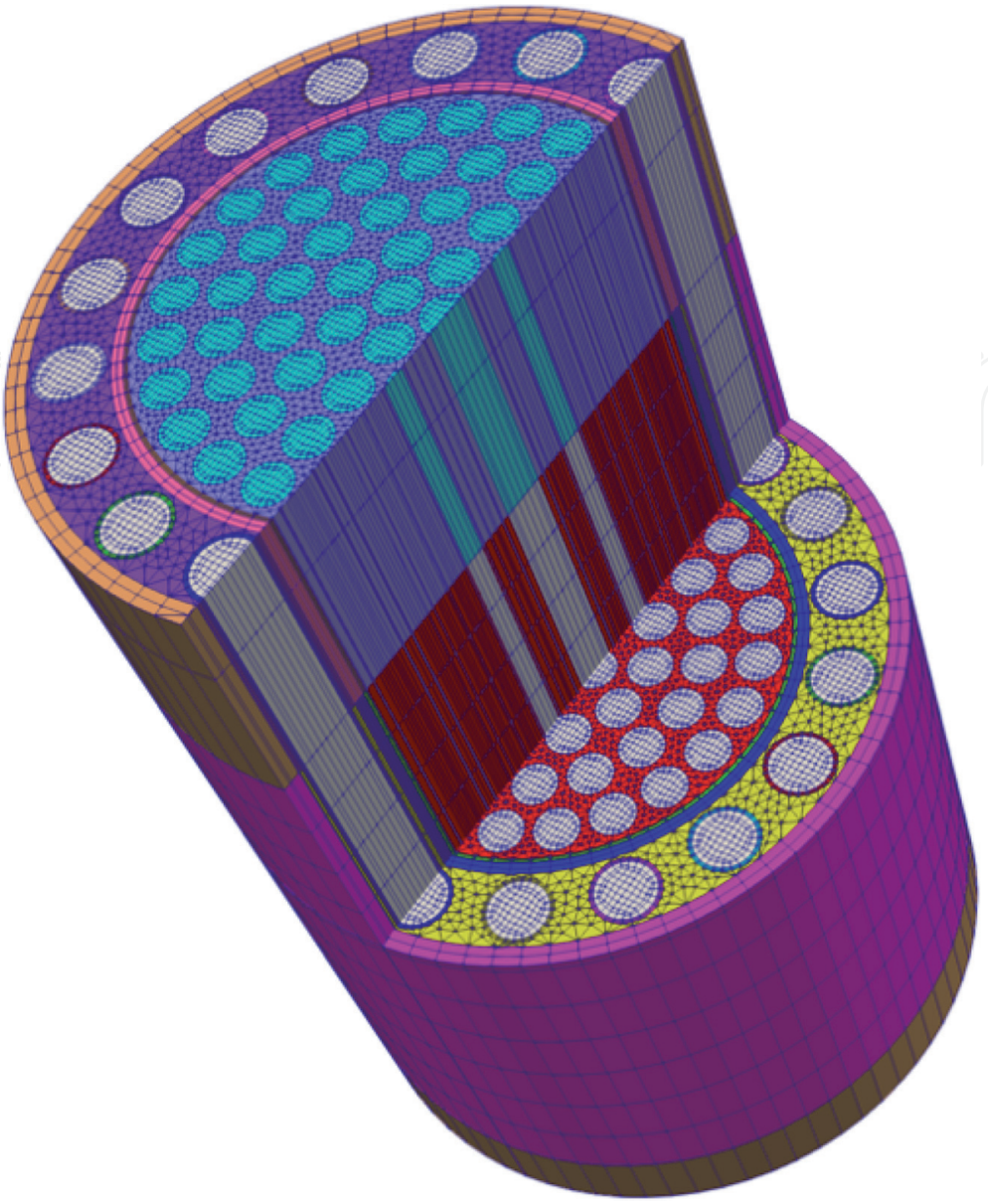

Figure 7.
Full-core neutronics and thermal meshes.

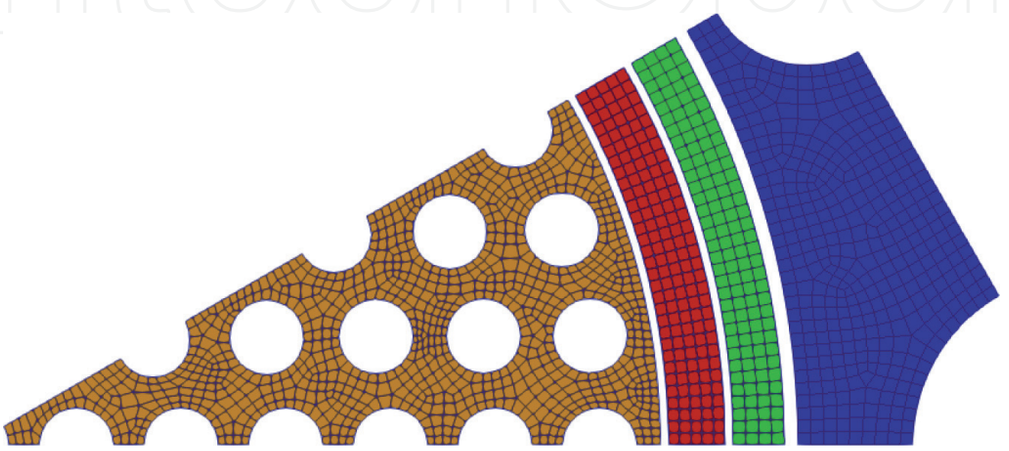

Figure 8.
X-Y view of the 30° slice thermal mesh.

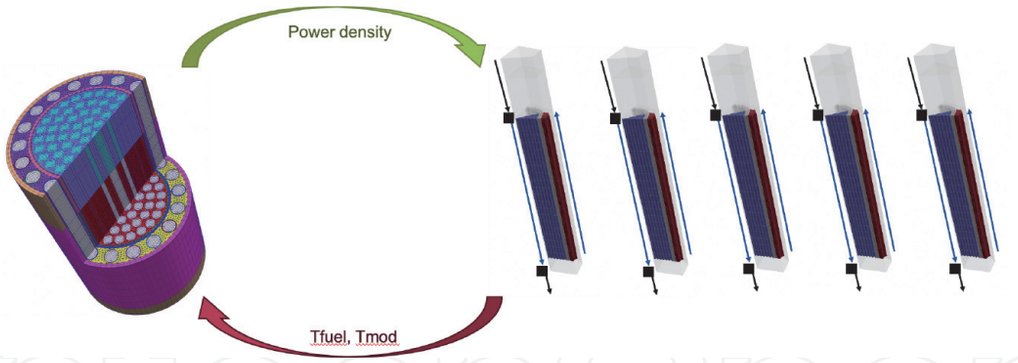

Figure 9.
Schematics of the full-core multiphysics model.

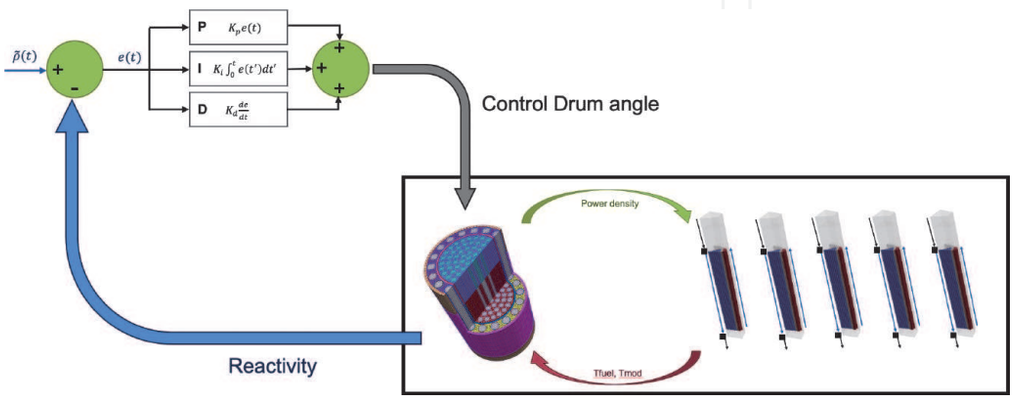

Figure 10.
Schematics of the PID control of the full-core multiphysics model.

corresponds to the reactivity computed by the numerical model with, for instance, an additional typical time delay from the detectors. An error between the desired and measured reactivity is then computed. The updated control drum angle is determined by adding three terms proportional to: (1) the error to attempt instantaneous correction; (2) the integral of the error to account for any persistent underestimating/overestimating of the desired reactivity; and (3) the derivative of the error to anticipate how it is going to evolve in the near-future and avoid overcorrection, with the controlling constants called K_p, K_i, and K_d, respectively.

The reason the reactivity is chosen to control the PID—rather than the power—is that a rotation of the drums induces an immediate reactivity change, whereas the corresponding power response is quite delayed (e.g., one may consider reactivity as being roughly the derivative of the power with respect to time). As such, it results in a much more stable control system. However, measured and desired power can be relatively easily converted to reactivity if the neutronic kinetics parameters of the reactor are well known.

The optimal values of K_p, K_i, and K_d can theoretically be determined if the transfer function for the system is known. However, given the complexity of the multiphysics model, it appears impractical to proceed that way. Instead, their values are chosen based on a semi-empirical approach. In particular, K_p represents the angle by which the drums are to be rotated per amount of reactivity. Fortunately, in most of the realistic operational range of the drums, the reactivity inserted per degree (α) is fairly constant and K_p can be approximately set to $1/\alpha$. If the error consistently lags behind the set point or tends to over-correct, the proper approach is to adjust K_i or K_d. In any event, the values of K_p, K_i, and K_d can be adjusted to make the system more or less responsive.

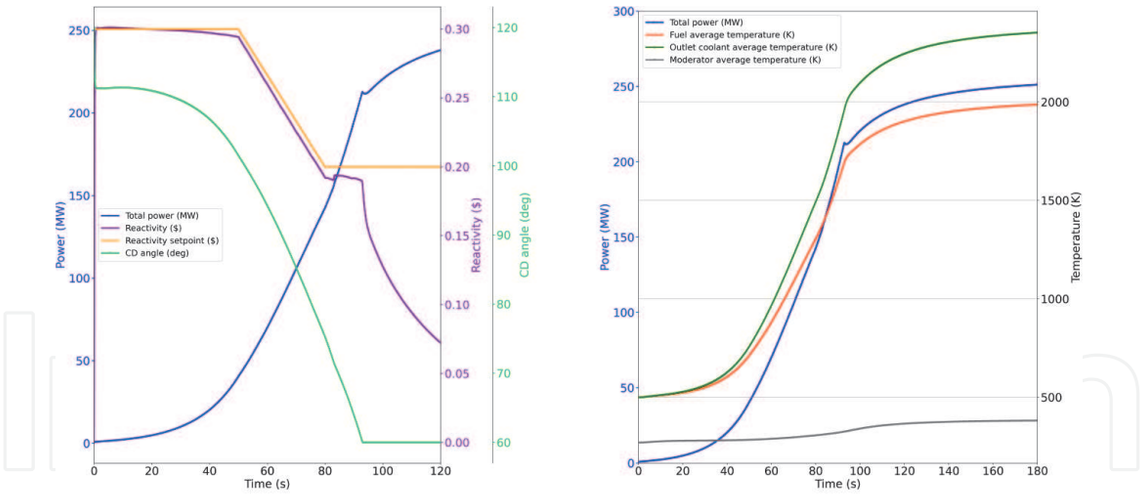

(a) (b)

Figure 11.
Reactivity setpoint, actual system reactivity, control drum actuation, power response, fuel average temperature, outlet coolant temperature, and moderator average temperature of the generic CERMET NTP system during the startup transient. (a) Reactivity control; (b) Core heating.

In the current simulations, the control system compensates the change in feedback accompanying the change in power well. During the simulation of a startup transient, the reactivity set point is chosen to be 0.3$ for the first 50 s, linearly ramping down to 0.2$ by 80 s of startup, and then remaining constant afterwards. The actual reactivity observed in the simulation closely follows the reactivity set point until the maximum control drum rotation is reached at about 100 s.

Reactor power increases from the initial 610 kW (10 kW per assembly) to close to 250 MW without over-swings in the completed simulation time. At around 90 s, a local maximum in the power is assumed that is attributed to the negative feedback outrunning control drum motion compensating for it. In this case, reactivity is under-compensated.

Temperatures increase monotonically throughout the transient with a corresponding temperature rise in the fuel, and outlet hydrogen being the largest at about 1500 K and moderator temperature rise being very small at less than 120 K. Increase in power will likely have to occur quicker in some NTP operational scenarios. It remains to be investigated if temperatures remain monotonic in these scenarios. The Griffin/RELAP-7/MOOSE model described herein is well equipped to investigate these scenarios (**Figure 11**).

5. Conclusions

This chapter has provided an overview of the concept of nuclear thermal propulsion for interplanetary travel. Nuclear thermal propulsion has a significant advantage in efficiency over current chemical rocket technologies, providing the opportunity to complete a trip to Mars in half the time previously anticipated, reducing exposure time for the spaceship crew. It also offers more options for mission abort if needed.

NTP was first conceived shortly after the end of World War II. Materials development programs and construction and operation of experimental facilities began in the 1950s under Project Rover, which was taken over by NASA shortly after its formation. Rover served as the basis for NASA's Nuclear Engine for Rocket Vehicle

Application (NERVA) program under Werner von Braun, and was planned to enable a mission to Mars, launching in the early 1980s. NERVA ended after funding cuts at the end of the Cold War and the corresponding reduction of the scope of the space program. However, this work was resurrected in the mid 2010s as part of NASA's Game Changing Technology for Deep Space Exploration Program. Much of the experience gained under NERVA was used as a basis for a path forward.

Under NERVA, fuel forms were primarily composed of graphite fuel compacts, although independent work at ANL and GE began developing CERMET fuels. Recent efforts picked up CERMET fuel development, building on the earlier work in addition to other research related to application in other reactor types. NASA also began the evaluation of CERCER fuel forms; all current development efforts are based on the use of HALEU fuel instead of the HEU fuel used within the NERVA program. Tests of fabrication processes and high temperature operation in reactor and non-reactor facilities are underway.

By using the Griffin reactor multiphysics application coupled with the RELAP-7 thermal-fluids systems code and the MOOSE framework, tightly coupled multiphysics simulations are being performed for CERMET-based core designs. The simulation of experiments being performed at the TREAT facility is also underway to aid in the experimental design. Data from the completed experiments are being used to validate the coupled approach.

Much work remains to be completed, both in core design analysis and materials testing to be able to build a prototype nuclear thermal rocket engine. NASA currently plans to launch a manned mission to Mars in 2039. According to a study commissioned by the National Academies of Sciences, Engineering, and Medicine [46], under such an aggressive time schedule, NTP development faces four major challenges: (1) the development of an NTP system that can heat its propellant to approximately 2700 K, which is the core exit for the duration of multiple burn cycles; (2) the need to rapidly bring an NTP system to full operating temperature in a very short time (e.g., on the order of a minute); (3) the long-term storage of LH_2 with minimal loss during a mission; and (4) the lack of U.S. testing facilities for system testing.

Acknowledgements

This work was funded under U.S. Department of Energy contract number DE-AC07-05ID14517, managed by Battelle Energy Alliance, LLC/Idaho National Laboratory for NASA's Space Nuclear Propulsion (SNP) project in the Space Technology Mission Directorate (STMD).

Nomenclature

α	Control drum reactivity inserted per degree of rotation [1/°]
c_p	Specific heat specific heat at constant pressure [J/(kg · K)]
c_v	Specific heat specific heat at constant volume [J/(kg · K)]
g_o	Gravitational constant on earth [m/s^2]
k	Ratio of c_p to c_v for propellant
K_p	PID proportional constant [°]
K_i	PID integral constant [°/s]
K_d	PID derivative constant [° · s]
I	Total impulse [N · s]

I_{sp}	Specific Impulse [s]
F_{thrust}	Force (thrust) exerted by propellant [N]
M	Molecular weight of propellant [g/mol]
m_{ex}	Total mass expelled over specific time [kg]
$\dot{m}$	Mass flow rate [kg/s]
T_c	Reactor core exit temperature for NTP or combustion chamber temperature for a chemical engine [K]
p_c	Core exit (or combustion chamber) pressure [N/m^2]
p_e	Nozzle exit pressure [N/m^2]
R	Univeral gas constant [J/kg · mol]
v_e	Exit velocity of propellant relative to nozzle [m/s]
W	Weight on earth [N]

Abbreviations

ATR	Advanced Test Reactor
ANL	Argonne National Laboratory
AEC	Atomic Energy Commission
CERCER	Ceramic–Ceramic
CERMET	Ceramic-Metal
GE	General Electric
GMWDF	Graphite matrix with dispersed fuel
HALEU	High Assay Low Enrichment Uranium
HEU	High Enrichment Uranium
HLLC	Harten, Lax, and Van Leer Contact
INL	Idaho National Laboratory
LASL	Los Alamos Scientific Laboratory
LEO	Low Earth Orbit
LEU	Low Enrichment Uranium
NASA	National Aeronautics and Space Administration
M&S	Modeling and simulation
MTFR	Moderator-to-fuel density ratio
MOOSE	Multiphysics Object Oriented Simulation Environment
NERVA	Nuclear Engine for Rocket Vehicle Application
NRC	Nuclear Regulatory Commission
NTP	Nuclear Thermal Propulsion
NTREES	Nuclear Thermal Rocket Element Environmental Simulator
PDE	Partial differential equation
PID	Proportional-Integral-Derivative
PRIME	Prototypic Reactor Irradiation for Multicomponent Examination
TREAT	Transient Reactor Test facility

DOI: http://dx.doi.org/10.5772/intechopen.103895

IntechOpen

Author details

Mark D. DeHart*, Sebastian Schunert and Vincent M. Labouré
Idaho National Laboratory, Idaho Falls, Idaho, United States of America

*Address all correspondence to: mark.dehart@inl.gov

IntechOpen

References

[1] Levack D, Horton J, Joyner C, Kokan T, Widman FW, Guzek B. Mars NTP architecture elements using the Lunar Orbital Platform-Gateway. In: Proceedings of the 2018 AIAA SPACE and Astronautics Forum and Exposition; 17–19 September 2018; Orlando, FL, USA. DOI: 10.2514/6.2018-5106

[2] National Aeronautics and Space Administration. Specific Impulse [Internet]. 2021. Available from: https://www.grc.nasa.gov/www/k-12/airplane/specimp.html [Accessed: 23 June 2021]

[3] Borowski SK. Nuclear thermal propulsion (NTP). In: Blockley R, Shyy W, editors. Encyclopedia of Aerospace Engineering. Available from. DOI: 10.1002/9780470686652.eae115 Accessed: 23 June 2021

[4] Joyner CR et al. LEU NTP engine system trades and mission options. Nuclear Technology; 2020;**206**(8): 1140-115. DOI: 10.1080/00295450.2019.1706982

[5] World Nuclear News. USNC subsidiary supporting cislunar rocket contractors [Internet]. 2021. Available from: https://world-nuclear-news.org/Articles/USNC-subsidiary-supporting-cislunar-rocket-contrac [Accessed: 23 June 2021]

[6] Stewart ME. A historical review of Cermet fuel development and the engine performance implications. In: Nuclear and Emerging Technologies for Space (NETS), 23 February 2015. Albuquerque, NM, USA. 2015. Available from: https://ntrs.nasa.gov/api/citations/20150002852/downloads/20150002852.pdf Accessed: 9 July 2021

[7] Emrich WJ Jr. Principles of Nuclear Rocket Propulsion. Oxford, UK: Butterworth-Heinemann; 2016

[8] Blagonravov AA, editor. Collected Works of K. E. Tsiolkovsky, Vol II: Reactive Flying Machines. A translation of "K. E. Tsiolkovskiy, Sobraniye Sochineniy, Tom II. Reaktivnyye Letatel' nyye Apparaty," Izdatel' stvo Akademii Nauk SSSR, Moscow, 1954. National Aeronautics and Space Administration, NASA TT F-237; Washington, DC. 1965

[9] Bennet J. NASA's nuclear thermal engine is a blast from the Cold War past. Popular Mechanics. 2018. Available from: https://www.popularmechanics.com/space/moon-mars/a18345717/nasa-ntp-nuclear-engines-mars/ Accessed: 21 September 2021

[10] National Aeronautics and Space Administration. Nuclear Thermal Propulsion: Game Changing Technology for Deep Space Exploration [Internet]. 2018. Available from: https://www.nasa.gov/directorates/spacetech/game_changing_development/Nuclear_Thermal_Propulsion_Deep_Space_Exploration [Accessed: 21 September 2021]

[11] Ruark AE, editor. Nuclear Powered Flight. APL/JEU-TG-20. Applied Physics Laboratory; Laurel, Virginia. 1947

[12] Spence RW. The Rover nuclear rocket program. Science. 1968;**160** (3831):953-959

[13] Houts MG, et al. NASA's nuclear thermal propulsion project. In: AIAA SPACE 2015 Conference and exposition. Pasadena, CA, USA, 31 August–2 September 2015. Available from: https://arc.aiaa.org/doi/abs/10.2514/6.2015-4523 [Accessed: 4 August 2021]

[14] DeHart MD, Karriem Z, Pope MA. Evaluation of the Enhanced LEU Fuel (ELF) design for conversion of the advanced test reactor to a low-enrichment fuel cycle. Nuclear Technology;**201**(3):247-266. DOI: 10.1080/00295450.2017.1322451

[15] Benensky K. Summary of Historical Solid Core Nuclear Thermal Propulsion Fuels. Report. Pennsylvania: The Pennsylvania State University; 2013. Available from: https://scholarsphere.psu.edu/resources/f44f5ad8-913d-4a0f-a8d4-337b29c6e021/downloads/479 Accessed: 2 September 2021

[16] Finseth JJ. Overview of Rover engine tests. Final report. Report. NASA-CR-184270. 1991. Available from: https://ntrs.nasa.gov/api/citations/19920005899/downloads/19920005899.pdf [Accessed: 2 September 2021]

[17] Koenig DR. Experience Gained from the space nuclear rocket program (Rover). Report. LA-10062-H. 1986. Los Alamos, New Mexico: Los Alamos National Laboratory; 1986. Available from: https://nuke.fas.org/space/la-10062.pdf [Accessed: 24 March 2022]

[18] Gaffin ND, Zinkle SJ, Palomares K. Review of irradiation hardening and embrittlement effects in refractory metals relevant to nuclear thermal propulsion applications. In: Nuclear and Emerging Technologies for Space (NETS-2019). American Nuclear Society Topical Meeting. Richland, WA, USA. 25–28 February 2019.

[19] Tucker DS. Cermets for use in nuclear thermal propulsion. In: Lucan D, editor. Advances in Composite Materials Development. London, UK: IntechOpen; 2019. DOI: 10.5772/intechopen.85220

[20] Burns D, Johnson S. Nuclear thermal propulsion reactor materials. In: Tsvetkov PV, editor. Nuclear Materials. London, UK: IntechOpen; 2020. DOI: 10.5772/intechopen.91016. Available from: https://www.intechopen.com/chapters/71396

[21] Schnitzler BG. Small Reactor Designs Suitable for Direct Nuclear Thermal Propulsion: Interim Report. Idaho Falls, Idaho: Idaho National Laboratory: 2012. DOI: 10.2172/1042384

[22] General Electric. 710 High-Temperature Gas Reactor Program Summary Report, Report GEMP-600-V1. Vol. I. Cincinnati, Ohio, USA: General Electric Co., Nuclear Materials and Propulsion Operation; 19681 DOI: 10.2172/4338293

[23] Venneri P, Kim YH, Howe S. Neutronics study on LEU nuclear thermal rocket fuel options. In: Proceedings of the KNS 2014 Fall Meeting. p. 1CD-ROM. Republic of Korea: KNS; 2014

[24] Tonks MR et al. Development of a multiscale thermal conductivity model for fission gas in UO_2. Journal of Nuclear Materials. 2016;**469**:89-98

[25] Ross SB, El-Genk MS, Matthews RB. Thermal conductivity correlation for uranium nitride fuel between 10 and 1923 K. Journal of Nuclear Materials. 1988;**151**(3):318-326

[26] Bhattacharyya, SK. An assessment of fuels for nuclear thermal propulsion. In: ANL/TD/TM01-22. Argonne, IL, USA: Argonne National Laboratory. December 2001. Available from: https://www.osti.gov/servlets/purl/822135 [Accessed: 4 August 2021]

[27] Argonne National Laboratory. Nuclear Rocket Program Terminal Report. ANL-7236. Lemont, Illinois: Argonne National Laboratory; 1966

[28] Nuclear Energy International. US NRC Approves Licence Amendment for Centrus to Produce HALEU [Internet]. 2021. Available from: https://www.neimagazine.com/news/newsus-nrc-approves-licence-amendment-for-centrus-to-produce-haleu-8827607 [Accessed: 6 August 2021]

[29] Houts M et al. Nuclear cryogenic propulsion stage. In: Nuclear and Emerging Technologies for Space (NETS-2014). Center, Mississippi: NASA Stennis Space; Feb. 24-26, 2014.

Available from: https://ntrs.nasa.gov/api/citations/20140012915/downloads/20140012915.pdf Accessed: 4 August 2021

[30] Schwartzberg FR, Ogden HR, Jaffee RI. Ductile-Brittle Transition in the Refractory Metals. Columbus, Ohio: Battelle Memorial Institute: Defense Metals Information Center; 1959. Available from: https://www.google.com/books/edition/Ductile_brittle_Transition_in_the_Refrac/eElxlohi01wC?hl=en&gbpv=1&pg=PP3 [Accessed: 24 March 2022]

[31] Gaffin N, Ang C, Milner J, Palomares K, Zinkle S. Fabrication of MO30W based cermets for nuclear thermal propulsion using spark plasma sintering. In: Nuclear and Emerging Technologies for Space (NETS 2021). American Nuclear Society Topical Meeting, Las Vegas, NV, USA. 26 February–1 March 2018.

[32] Poston D. Design comparison of nuclear thermal rocket concepts. In: Nuclear and emerging Technologies for Space (NETS 2018). American Nuclear Society Topical Meeting; Oak Ridge, TN, USA; 26–30 April 2021

[33] Youinou GJ, Lin CS, Abou Jaoude A, Casey JJ. Nuclear thermal propulsion scoping analysis of fuel plate core configurations. In: INL/EXT-19-57004. Idaho Falls, ID, USA: Idaho National Laboratory; 2020. DOI: 10.2172/1596107

[34] Gustafson JL. Space nuclear propulsion fuel and moderator development plan conceptual testing reference design. Nuclear Technology. 2021;**207**(6):882-884. DOI: 10.1080/00295450.2021.1890991

[35] Braun R et al. Space nuclear propulsion for human Mars exploration. In: NASEM Space Nuclear Propulsion Technologies Committee Report. Washington, DC: National Academies of Sciences, Engineering and Medicine; 2021. DOI: 10.17226/25977

[36] Benensky K. Tested and Analyzed Fuel Form Candidates for Nuclear Thermal Propulsion Applications. Nuclear Engineering Reports: University of Tennessee; 2016. Available from: https://trace.tennessee.edu/utne_reports/5 Accessed: 24 August 2021

[37] Poston D. Nuclear testing and safety comparison of nuclear thermal rocket concepts. In: Nuclear and emerging Technologies for Space (NETS 2018). Las Vegas, NV, USA: American Nuclear Society Topical Meeting; 26 Feb–1 Mar, 2018

[38] Duderstadt JJ, Hamilton LJ. Nuclear Reactor Analysis. Wiley: New York, NY, USA; 1976

[39] Proust E. Lecture Series on Space Nuclear Power and Propulsion Systems-2-Nuclear Thermal Propulsion Systems (last updated in January 2021). DOI: 10.13140/RG.2.2.17073.10089

[40] Black DL. Consideration of low enriched uranium space reactors. In: AIAA 2018-4673. AIM Propulsion and Energy Forum, July 9-11, 2018, Cincinnati, Ohio: 2018 Joint Propulsion Conference; July 9-11, 2019

[41] Bae IH, Na MG, Lee YJ, Park GC. Calculation of the power peaking factor in a nuclear reactor using support vector regression models. Annals of Nuclear Energy. 2008;**35**(12):2200-2205

[42] Zabriskie AX et al. A coupled multiscale approach to TREAT LEU feedback modeling using a binary-collision Monte-Carlo–informed heat source. Nuclear Science and Engineering. 2019;**193**(4):368-387. DOI: 10.1080/00295639.2018.1528802

[43] Schnitzler B, Borowski S, Fittje J. A 25,000-lbf thrust engine options based

on the small nuclear rocket engine design. In: AIAA 2009-5239. 45th AIAA/ASME/SAE/ASEE Joint Propulsion Conference and Exhibit. Denver, Colorado. August 2009

[44] Fittje JE, Borowoski SK, Schnitzler BG. Revised point of departure design options for nuclear thermal propulsion. In: AIAA 2015-4547. AIAA SPACE 2015 Conference and Exposition, Pasadena, CA, USA. August 2015. Available from: https://arc.aiaa.org/doi/10.2514/6.2015-4547 [Accessed: 10 August 2021]

[45] Nam SH et al. Innovative concept for an ultra-small nuclear thermal rocket utilizing a new moderated reactor. Nuclear Engineering and Technology. 2015;**47**(6):678-699

[46] National Academies of Sciences, Engineering, and Medicine. Space Nuclear Propulsion for Human Mars Exploration. Washington, DC, USA: The National Academies Press; 2021. DOI: 10.17226/25977

[47] Los Alamos National Laboratory. N-Division Personnel. Pewee I Reactor Test Report. Los Alamos National Laboratory Informal Report, LA-4217. Los Alamos, NM, USA: Los Alamos National Laboratory; 1969

[48] Stacy WM. Nuclear Reactor Physics. New York, NY, USA: Wiley; 2007

[49] Gates JT, Denig A, Ahmed R, Mehta VK, Kotlyar D. Low-enriched cermet-based fuel options for a nuclear thermal propulsion engine. Nuclear Engineering and Design. 2018;**331**:313-330. DOI: 10.1016/j.nucengdes.2020.110605

[50] Krecicki M, Kotlyar D. Low enriched nuclear thermal propulsion neutronic, thermal hydraulic, and system design space analysis. Nuclear Engineering and Design. 2020;**363**:110605

[51] Walton JT. An overview of tested and analyzed NTP concepts. NASA Technical Memorandum 105252, AIAA-91-3503, Conference on Advanced Space Exploration Initiative Technologies, cosponsored by AIAA, NASA, and OAI, Cleveland, Ohio, September 4-6, 1991. Available from: https://ntrs.nasa.gov/api/citations/19920001919/downloads/19920001919.pdf [Accessed: 24 March 2022]

[52] Permann CJ et al. MOOSE: Enabling massively parallel multiphysics simulation. SoftwareX. 2020;**11**:100430. Available from: https://www.sciencedirect.com/science/article/pii/S2352711019302973 [Accessed: 24 March 2022]

[53] Kirk BS, Peterson JW, Stogner RH, Carey GH. libMesh: A C++ library for parallel adaptive mesh refinement/coarsening simulations. Engineering with Computers. 2006;**22**(3–4):237-254. DOI: 10.1007/s00366-006-0049-3

[54] Balay S, et al. PETSc Users Manual. ANL-95/11 Rev 3.7. 2016. Available from: https://ntrs.nasa.gov/api/citations/20140012915/downloads/20140012915.pdf [Accessed: 1 November 2021]

[55] Martineau R et al. Multiphysics for nuclear energy applications using a cohesive computational framework. Nuclear Engineering and Design. 2020; **367**:110751. DOI: 10.1017

[56] Wang Y et al. Rattlesnake: A MOOSE-based multiphysics multischeme radiation transport application. Nuclear Technology;**207**(7): 1047-1072. DOI: 10.1080/00295450.2020.1843348

[57] Wang Y et al. Performance improvements for the Griffin transport solvers. In: INL/EXT-21-64272-Rev000. Idaho Falls, ID, USA: Idaho National Laboratory; 2021. Available from: https://inldigitallibrary.inl.gov/sites/sti/sti/Sort_50897.pdf [Accessed: 15 September 2021]

[58] Shemon ER et al. PROTEUS-SN User Manual, Revision 1.2. ANL/NE-14/6. Chicago, IL, USA: Argonne National Laboratory; 2014

[59] Lee CH et al. MC2-3: Multigroup cross-section generation code for fast reactor analysis. In: ANL/NE-11/41, Rev. 3. Chicago, IL, USA: Argonne National Laboratory; 2018

[60] Schunert S et al. Control rod treatment for FEM based radiation transport methods. Annals of Nuclear Energy. 2019;**127**:293-302

[61] Williamson RL et al. BISON: A flexible code for advanced simulation of the performance of multiple nuclear fuel forms. Nuclear Technology;**207**(7):954-980. DOI: 10.1080/00295450.2020.1836940

[62] Hirschhorn J et al. Review and preliminary investigation into fuel loss from cermets composed of uranium nitride and a molybdenum-tungsten alloy for nuclear thermal propulsion using mesoscale simulations. Journal of Materials. 2021;**73**(11):3528-3543. DOI: 10.1007/s11837-021-04873-x. Available from: https://link.springer.com/content/pdf/10.1007/s11837-021-04873-x.pdf [Accessed: 24 March 2022]

[63] Berry RA et al. RELAP-7 Theory Manual. INL/EXT-14-31366, Rev. 2. Idaho Falls, ID, USA. Available from: https://inldigitallibrary.inl.gov/sites/sti/sti/6899506.pdf: Idaho National Laboratory; 2016 Accessed: 15 September 2021

[64] Adhikary D, Jayasundara C, Podgorney R, Wilkins A. A robust return-map algorithm for general multisurface plasticity. International Journal for Numerical Methods in Engineering. 2017;**109**(2):218-234. DOI: 10.1002/nme.5284

[65] Wang Y, et al. Demonstration of MAMMOTH strongly-coupled multiphysics simulation with the Godiva benchmark problem. In: M&C 2017 - International Conference on Mathematics & Computational Methods Applied to Nuclear Science & Engineering, Jeju, Korea, April 16-20, 2017. Available from: https://www.kns.org/files/int_paper/paper/MC2017_2017_9/P353S09-01WangY.pdf [Accessed: 24 March 2022]

[66] Klein AC, Camp AL, PR MC, Voss SS. Operational Considerations for Fission Reactors Utilized on Nuclear Thermal Propulsion Missions to Mars—A Report to the Nuclear Power & Propulsion Technical Discipline Team. NASA Technical Report NASA/CR20210000387. Hampton, VA, USA: Langley Research Center; Jan 2021

[67] Xia Y et al. Preliminary Study on the Suitability of a Second-order Reconstructed Discontinuous Galerkin Method for RELAP-7 Thermal-Hydraulic Modeling. INL/EXT-17-43108-Rev001. Idaho Falls, ID, USA: Idaho National Laboratory; 2017. DOI: 10.2172/1468483

[68] Labouré V et al. Hybrid super homogenization and discontinuity factor method for continuous finite element diffusion. Annals of Nuclear Energy. 2019;**128**:443-454. DOI: 10.1016/j.anucene.2019.01.003

[69] Leppänen J et al. The serpent Monte Carlo code: Status, development, and applications in 2013. Annals of Nuclear Energy. 2015;**82**:142-150. DOI: 10.1016/j.anucene.2014.08.024